Date of publication xxxx 00, 0000, date of current version xxxx 00, 0000.

Digital Object Identifier 10.1109/ACCESS.2017.DOI

Multi-view data augmentation to improve wound segmentation on 3D surface model by deep learning

R. NIRI[1], E. GUTIERREZ[2], H. DOUZI[1],Y. LUCAS[3], S. TREUILLET[3], B. CASTANEDA[2], and I. Hernandez[4].

[1]IRF-SIC LaborNacional ory, Ibn Zohr University, Agadir, Morocco.
[2]Department of Engineering, Pontifical Catholic University, Lima, Peru.
[3]PRISME Laboratory, Orleans University, Orleans, France.
[4]Hospital Nacional Hipolito Unanue, Lima, Peru.

Corresponding author: R. Niri (e-mail: rania.niri@edu.uiz.ac.ma).

This work was supported by the European Union's Horizon 2020 under the Marie Sklodowska-Curie grant agreement No 777661.

ABSTRACT Wound area segmentation really progressed with the emergence of deep learning, due to its robustness in uncontrolled lighting and no need to design hand-crafted features but two limits have still to be overcome : firstly, its performance relies on the size and quality of the training dataset in the medical field, where data annotation is costly and time-consuming ; secondly the accuracy of the segmentation depends highly on the camera distance and angle and moreover perspective effects prevent measuring real surfaces in single views.

To address concurrently these two issues, we propose to apply multi-view modeling : an image sequence is acquired around the wound site and enables wound 3D reconstruction. Then, a segmentation step is run to extract roughly the wound from the background in each view and to select the best view with an original strategy. This view provides the most accurate segmentation and the real wound bed area even on non planar wounds. Finally, this segmentation is backprojected in each view to generate a complete set of well annotated real images to reinforce the learning step of the neural network.

In our experiments, we compare several strategies to select the best view in the image sequence. The proposed method, tested on a dataset of 270 images, outperforms standard deep learning approach based on a single view, as recorded with DICE index and IoU score which rise respectively from 36.53% to 86.3% and 29.48% to 77.09% for the wound class to achieve an overall DICE and IoU score of 93.04% and 86.61% including background class. These results attest to the robustness of our method and its improved accuracy in the wound segmentation task.

INDEX TERMS Deep Learning, 3D Registration, Chronic Wounds, Semantic Segmentation, Data Augmentation, U-Net

I. INTRODUCTION

CHRONIC wounds are a major health issue that affect population quality of life and lead to a huge burden for the healthcare systems worldwide [1]. Chronic wounds include venous ulcers, pressure injuries, diabetic ulcers, traumatic and surgical ulcers, etc. These wounds are complex and heal gradually depending on their severity. Wound healing process is a complicated procedure that requires regular checkups by wound specialists. The fundamentals of a successful clinical care require trained clinicians with fast decision making. Tracking wound size including length, width, depth, and circumference is a key indicator to enable healing and evaluate response to treatment.

There are various methods to assess the healing progress, most commonly, practitioners use rudimentary modalities to measure the surface area such as simple rulers or wound outline tracing [2] [3] [4]. Even more, a moldable material or a cotton tipped swab are inserted inside the wound cavity to measure the volume and depth [5]. These manual methods are often harmful, time consuming and require wound contact which can carry high risk of infection. In addition, the accuracy of these techniques relies on the subjective diagnosis of

clinicians depending on their prior experience [6]. However, for a relevant wound assessment, it is vital that the ideal measuring tool must be unbiased, accurate and consistent.

Over the last years, the application of photography became increasingly popular in clinical practice. It avoids direct wound contact and enable clinicians to achieve more consistent and accurate wound assessment. More recently, smartphone wound image analysis have been extensively used to assist clinicians in qualitative diagnosis. Smartphones are low-cost, noninvasive, user-friendly and are already equipped with high-resolution cameras.

2D imaging measurements can be greatly affected by body curvature, wounds are not planar and perspective distortion affects area estimation [7]. Also, a single view does not provide volume and depth information that are essential to perform an accurate chronic wound monitoring. 3D imaging techniques overcomes the shortcomings and limitations of 2D methods. 3D methods have been introduced to improve assessment in different medical areas [8]. They provide a more accurate evaluation of wounds than a simple 2D approach [5]. Existing 3D scanning devices are actually expensive and not adapted to the clinical practice. In contrast, two or more converging pairs of views can be used to reconstruct the 3D surface area of the wound using a smartphone camera and a simple multi-view approach based on Structure from motion (Sfm). The reconstructed 3D model can be monitored from any angle and perspective. In addition, the obtained 3D point clouds can offer much more detailed information about the lesion regardless of the wound position and size.

Background segmentation is an essential step in photography based wound analysis because it influences the outcome of the entire assessment process (area, perimeter, etc). The segmentation in the 3D model is obtained from the 2D segmentation of each image using scene fusion. 2D segmentation is performed using DL, then the results are directly mapped on the mesh surface of the 3D model. Thus, it is important to perform an accurate DL segmentation of the 2D images to obtain a precise wound delineation in the 3D model. However, despite the success of DL in many wound segmentation applications, there is a major limitation of these DNN. To obtain good performance a massive number of annotated images is required for training. Indeed, this is extremely cost-effective and expert-intensive in the field of medical image analysis.

One of the most common techniques to overcome the lack of training images is data augmentation, where images are created virtually using different processing methods like translation, flipping, rotation, scaling, etc. Nevertheless, these techniques alter original wound shape characteristics, so the produced images do not represent the real appearance of the wound area. The same wound could greatly vary in shape using a simple data augmentation technique by rotation or translation. Thus, we propose a weakly supervised data augmentation technique that includes all the aspects of the wound from different point of views using real images. The main idea is to capture multiple views of the wound by moving the camera around it; to the left, right, up and down. Then an automatic segmentation of these images using a pretrained DNN could be used as annotations to extend the training set. Hence, an accurate DL segmentation of all the views is primordial. The same image sequence will be used to obtain the segmentation of the wound in the 3D model.

However, DL is rather sensitive to camera distance and shooting angle. To produce a correct segmentation, the image has to be taken perpendicularly to the wound surface, what we call a frontal view. In addition, the wound should be located in the center of the image and with a distance not too close nor far from the camera. If the angle or the distance from the wound is slightly changed from a view to another one, the accuracy can quickly decrease, especially for large or highly curved lesions. Moreover, for small size wounds, DL fails completely to segment the non-frontal views.

To this end, we propose a novel DL based wound segmentation method that overcomes large angles and distance variation using best view selection and 3D model reconstruction. The method goes through several steps: (1) semantic segmentation of the 2D image sequence using a pretrained network (2) 3D model reconstruction and best view selection (3) reprojection of the best view segmentation on each image of the multi-view sequence. The obtained masks could be used to extend the training set and they can also be mapped on the mesh surface of the 3D model to obtain a robust 3D segmentation.

We evaluated our method by conducting comprehensive experiments. We focused our experiments on diabetic foot ulcers as they combine chronic wounds characteristics, ischemia and infection [9]. The proposed method provides more precise and robust segmentation from any viewing angle and distance. Moreover, it is applicable to all wound types from the largest to the smallest ones regardless of their location and healing stage.

The rest of the paper is structured as follows. In Section II, a brief literature review on 2D wound segmentation methods is provided followed by recent approaches for 3D model reconstruction. Section III describes in details the complete methodology proposed in this paper. In Section IV, segmentation results are shown and analyzed followed by a discussion of our major experiments in Section V. Finally, in Section VI, we conclude and suggest some directions for future work.

II. LITERATURE REVIEW

A. WOUND SEGMENTATION

Prior to the rise of deep learning in medical imaging, wound segmentation mostly relied on machine learning algorithms [16] [17] [18] and [10]. These methods generally use classifiers such as SVM which have the advantage of not being very data intensive. However, they require hand-crafted features to extract color and texture descriptors. Moreover, they suffer from a poor generalization in uncontrolled lighting environments. These problems were resolved by using deep learning networks (DNN). Recent research works have focused on DNN to address wound segmentation task using

TABLE 1. Contribution comparison with related works

	Gholami [10]	Liu [11]	Wang [12]	QTDU [13]	ASURA [14]	Zahia [15]	Ours
Wound Segmentation	✓	✓	✓	✓	✓	✓	✓
PixelWise Segmentation			✓	✓	✓	✓	✓
Deep Learning based			✓	✓	✓	✓	✓
Small Dataset	✓	✓				✓	✓
Smartphone based 2D to 3D surface segmentation		✓					✓

convolutional neural networks (CNN) or fully convolutional networks (FCN).

Alzubaidi et al. [19] developed a novel deep convolutional neural network named DFU_QUTNet for diabetic foot skin classification (normal and abnormal skin). Features extracted by DFU_QUTNet were used to train SVM and KNN classifiers. While Goyal et al. [20], trained a Faster R-CNN with Inception V2 using two-tier learning with the MS COCO dataset. Their objective was to detect DFU localization using a relatively small dataset of DFU images. A post-processing step was required to improve the results. In a recent work [12], they performed foot ulcer segmentation using a light-weight convolutional framework based on MobileNetV2 and connected component labelling using a dataset consisting of 1109 foot ulcer images. Newer methods with EfficientDet [21] provided superior ulcer detection accuracy during MICCAI conference challenge using DFUC 2020 dataset [22]. This dataset consists of 4500 diabetic foot ulcer images with expert annotations. Although the proposed methods were highly accurate in wound localization [23] [24], both studies did not address wound segmentation precision and wound area measurement. Among the biggest limitation of these methods is that thousands of annotated images are required to attain such a good performance, a requirement that is costly and difficult to satisfy in the medical field. To deal with the massive training data requirement in DL, many researchers used data augmentation and transfer learning [25]. Also, other researchers adopted hybrid methods combining neural networks and ML classifiers.

Wound segmentation on 3D surface model is commonly used to improve the performance of the 2D segmentation method. It helps to enhance wound detection from various angles and distances independently of their size and shape. To the best of our knowledge, there is a very limited number of works that have addressed wound segmentation on 3D surface using only smartphone images and DL techniques. Liu et al. [11] proposed a method with 3D transformation to measure wound area which implements 3D reconstruction based on SFM, then LSCM was used to unwrap the UV map of the 3D model. However, image segmentation was performed by an interactive method which is time consuming and relies on the experience of medical experts. Thus, the authors state that an automatic segmentation method using DL should be considered in the future to improve wound extraction and measurement. In another paper, Zahia et al. [15] proposed a DL based method using Mask RCNN to perform wound segmentation on the 3D mesh. Although they achieved good results, their method requires Structure Sensor 3D scanner to obtain the 3D reconstruction from smartphone images. In this paper, we propose an end-to-end DL based system for wound segmentation on 3D model surface using smartphone images without any other equipment for 3D model reconstruction. Table 1 summarizes a comparison of related survey papers addressing wound segmentation against our proposed method.

B. 3D MODEL CREATION

Given the disadvantages of traditional wound assessment, technology that uses imaging to perform non-contact measurements began to increase in popularity in the 1990s. In particular, 3D measurements of wound characteristics become popular as more accurate and precise information can be obtained than with the use of 2D imaging. [26]–[28].

In the creation of 3D models, two methodologies can be distinguished: active and passive reconstruction. Active approach consists on sending a signal to the object of interest to obtain accurately the depth and building 3D structure from there. Devices using this approach are usually fast and can offer high accurate results but are also expensive and might require complex settings. Laser scanners and structured light 3D scanners are examples of technologies using active approach and have demonstrated accurate results for wound measurements. [29] reports less than 2% errors and less than 4% precision rates error for volumetric calculations based on laser scanner when compared to traditional manual methods. Additionally, Darwig et al. [30] presented a 3D-scanners based on active approach with no significant difference on area measurements compared to using laser scanners.

Passive methods, on the other hand, are methods in which no signal interferes with the object. They only require images from digital cameras to infer the 3D point cloud and therefore are less expensive and complex to use than active approach devices. In particular, Structure from motion (SfM) is an attractive technique as it only requires a single digital camera and is available in several free software packages.

Previous studies demonstrate SfM can be useful for wound assessment: In [31], a methodology based on SfM was shown to be useful for wounds with precision of volumetric measurements around 3%. On the other hand, [32] and [33], demonstrate that SfM 3D models are repeatable and consistent with laser scan 3D results: the registration error between SfM and laser scan-based 3D models is on average less

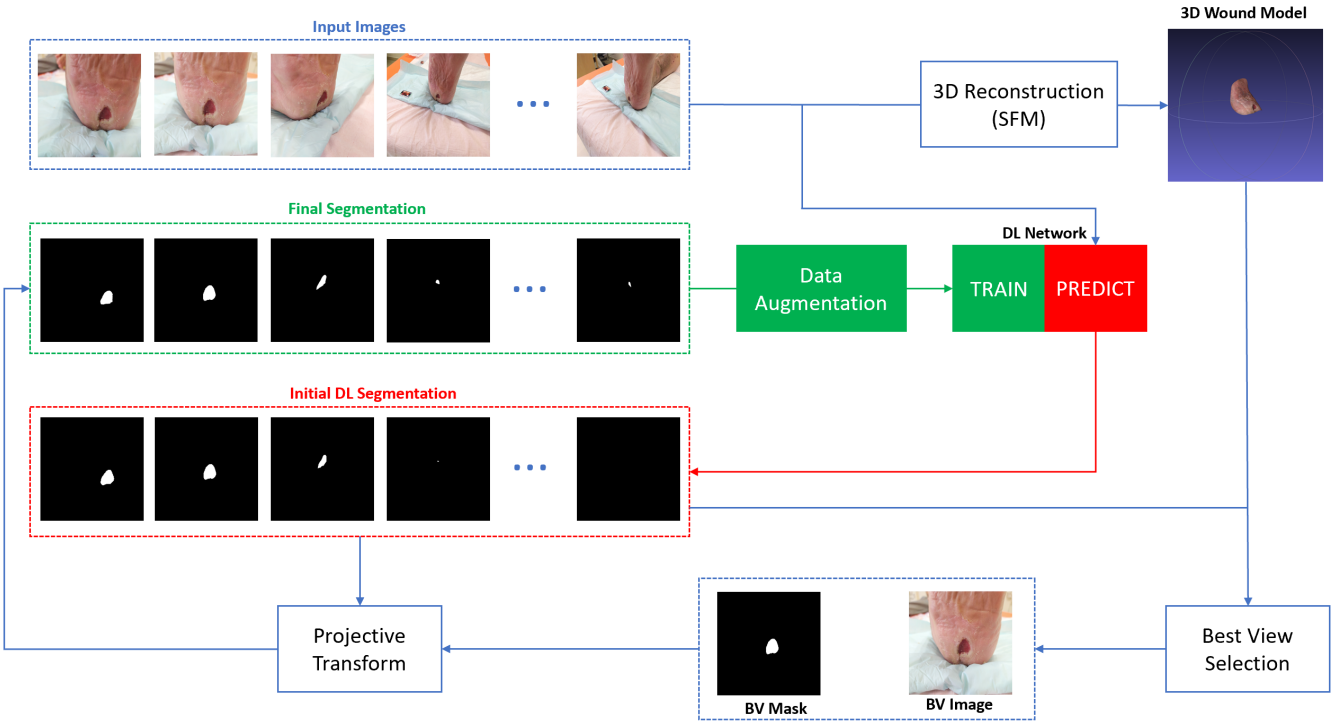

FIGURE 1. Workflow of the proposed 3D based segmentation method using DL and BV selection

than 1mm. In addition, the potential for using SfM increases given the capabilities currently found in smartphone's CPU and GPU. Recent studies have shown that SfM can be fully implemented in smartphones [34] [35].

III. METHODOLOGY

Our contribution can be summarized as follows (See Figure 1) :

1) A robust wound segmentation method with an effective background removal using DL.
2) 3D model reconstruction using a simple acquisition protocol with a monocular camera from a low-cost smartphone and using SfM to infer the 3D structure.
3) A novel pipeline of wound segmentation that overcomes large angles and distance variation using camera view selection and 3D model reconstruction.
4) Experiments and analyses on various diabetic foot ulcers with different sizes and location that demonstrate the effectiveness of our method.

A. ROBUST WOUND SEGMENTATION

We built an annotated database consisting of 569 chronic wound images covering all pathologies such us diabetic foot ulcers, burns, pressure injuries, etc, mostly captured from a relatively perpendicular angle. This dataset contains various wounds with distinct size and in different healing stages. The images were taken in several medical sites with different cameras and without any strict protocol regarding lighting conditions. Consequently, the segmentation task was quite challenging. Most images have different backgrounds including lots of regions similar to the wound bed which may threaten the segmentation. Indeed, segmenting chronic wounds demands a high level of accuracy, small marginal segmentation errors can lead to wrong measurements and poor user experience in clinical settings. To this end, we propose a robust wound segmentation method comprising wound delineation and skin correction for an effective background removal without increasing the complexity of deep neural networks.

To perform wound delineation, we based our segmentation on our previous work [36] while proposing more robust background elimination using skin correction. We opted for the state-of-the-art semantic segmentation network U-net for medical images [37]. U-net has proven to be very powerful specifically in the field of biomedical images segmentation using few data. Our method consists of two main stages (See Figure 2).

First, wound area extraction which aims to eliminate all background elements. Second, the obtained wound segmentation mask will be post-processed by skin detection algorithm. Its goal is to remove all background non-skin pixels. Thus, only segmented elements inside skin area will be conserved. When skin segmentation map is combined with the wound map, we are able to provide more accurate segmentation. Finally, the generated mask is further refined by hole filling and the removal of missing small points in the segmentation map using morphological operations (i.e., erosion, dilation, opening and closing) [38].

To perform robust 2D segmentation, the database was divided into training and testing set. The partition percentage

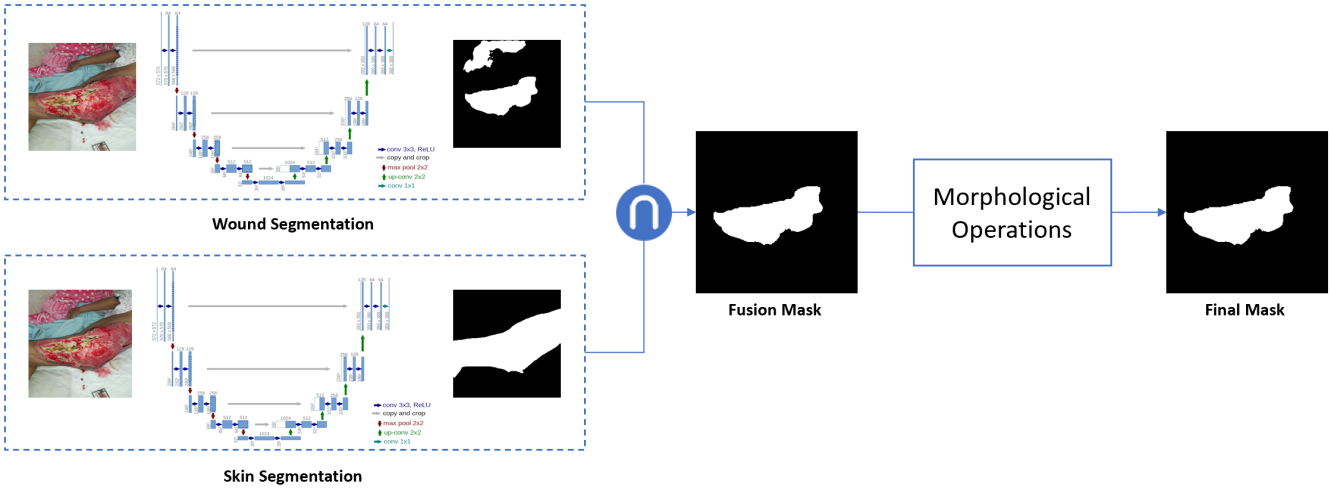

FIGURE 2. 2D chronic wound segmentation pipeline

was around 75% and 25% respectively. Both U-net networks for wound and skin segmentation tasks were trained for 200 epochs and were implemented in Keras with TensorFlow backend using the Adam optimization algorithm [39] with a learning rate of 0.001. The performance of the proposed segmentation procedure helped to improve the accuracy to reach a Jaccard index of 98.48% and a Dice score of 99.26% instead of 94.96% and 97.25% in the previous version [36] using the same testing set. The proposed 2D segmentation method overcomes perfectly complex background elimination and uncontrolled lighting conditions, but it still can be greatly affected by high angle and distance variation due to camera position and orientation in the image sequence.

B. 3D MODEL CREATION

Given the advantages in terms of required devices and portability, SfM has been selected for 3D model creation in this study.

The 3D model of a wound requires images from different viewpoints of a static scene. Therefore, patients are asked to rest in a comfortable position. A card with a colored pattern is placed near the wound to adjust the size of the digitized 3D model. Next, the smartphone camera is placed between 10 and 20 cm in front of the wound in focus and acquisition is started. By manually moving the camera in a circular motion around the wound for 1 minute, about 40 photos are acquired.

The 3D modeling pipeline starts with a SIFT feature extraction and matching after which the structure-from-motion algorithm is used to infer the 3D structure. A sparse point cloud is created to sketch the 3D model. Next, the Semi-Global Matching (SGM) algorithm is used to create depth maps in order to create a dense 3D point cloud and triangulated surface on which texture is superimposed. As a final step, a Laplacian filter is applied to reduce noise that may appear during the reconstruction of the dense 3D model.

The described process for creating the 3D mesh is performed using an open source software: Alicevision [40] which is possible to run automatically through Python. Figure 3 shows the pipeline based on SfM for the 3D mesh creation.

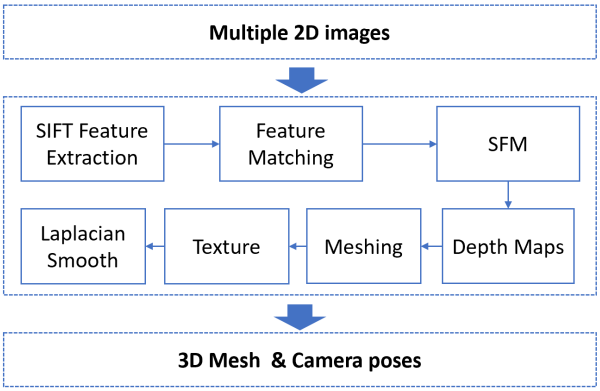

FIGURE 3. 3D model creation pipeline

As a result of this process, we obtain a dense 3D mesh for the different views to relate the 2D segmentation to the 3D model.

C. WOUND SEGMENTATION ON THE 3D SURFACE MODEL

Since each DL segmentation mask can produce a different outline of the wound in the 3D model, the distance and angle between the wound surface and the camera is used to select the most appropriate view. The distances and angles are calculated as follows:

1) The 3D model is projected onto the camera plane and using the corresponding DL segmentation mask, the temporal segmentation of the wound is created in the 3D model.
2) From the point cloud corresponding to the wound

FIGURE 4. Sample of best view selection in the multi-view sequence

surface, the Euclidean distance between each point and the center of the camera is calculated.

3) For each triangle on the wound surface, the angle between the principal camera ray and the normal of each triangle is calculated.
4) Finally, we use the median of the distances and the median of the angles calculated above to summarize the relative position of each camera with respect to the wound.

D. BEST VIEW SELECTION

Four strategies are used to select the most appropriate camera view. For this, the relative position of each camera to the wound calculated above is used. The selected view is respectively:

- Strategy 1: The view with the most acute camera-to-wound angle.
- Strategy 2: The view with the closest camera-to-wound distance .
- Strategy 3: The view with the closest distance within the 5 images with the sharpest camera-to-wound angles.
- Strategy 4: The view with the most acute angle among the 5 images with the closest distances between camera and wound.

In Figure 4, the selection of a view with the strategy 3 is shown as an example.

E. 3D MODEL SEGMENTATION AND POST-PROCESSING

After selecting an appropriate view with one of the 4 strategies, the corresponding segmentation mask is used to create the final segmentation of the wound in the 3D model. This segmentation is combined with a post-processing of the 3D mesh to smooth the wound edges which consists of subdividing the wound contour in the 3D mesh and using a simple neighbor averaging based on a wound indicator to obtain a smoothed wound contour.

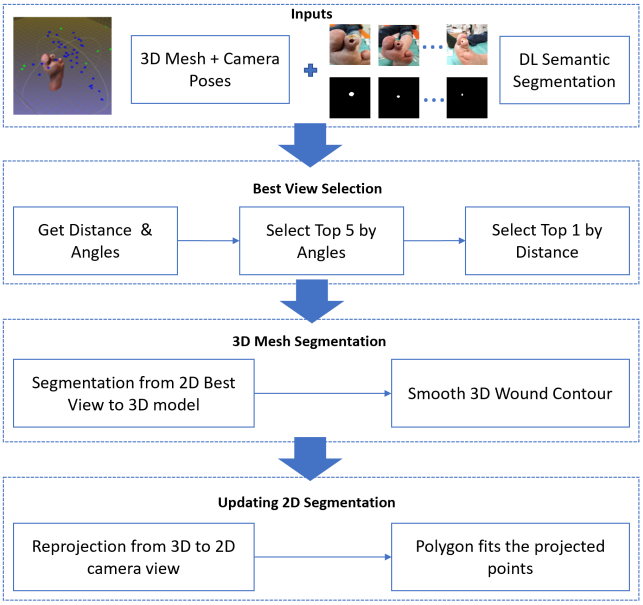

FIGURE 5. Workflow of the 3D model re-projection to update semantic segmentation

Finally, the wound segmentation resulting from the above process is projected onto the corresponding views of all 2D images. The result is a collection of updated 2D segmentation masks. Figure 5 shows the complete process performed to create the 3D mesh segmentation and update the semantic segmentation on the 2D images with the proposed methodology.

IV. RESULTS

A. DATASET AND MATERIAL

In cooperation with the diabetology service of the CHRO (Regional Hospital of Orleans in France), we collected a second data set of 270 diabetic foot images taken from 7 patients during multiple clinical visits. The images were captured using a Xiaomi Note7 smartphone. The acquisition protocol includes several points of views with different viewing angles and distances for each wound.

For creating the ground truth labels, the wounds are manually delineated directly on the 3D model using MeshLab then reviewed and verified by wound care experts. The segmented 3D model is then projected onto each of the camera views and the corresponding wound segmentation masks are obtained for each single view.

B. METRICS

To evaluate the segmentation performance, four metrics were adopted. Dice Similarity Coefficient (DICE) and Intersection Over Union (IoU) were used to quantify the overlap between the obtained segmentation mask and the ground truth. While Root Mean Square Error (RMSE) and Mean Absolute Error (MAE) were used to measure the difference per pixel between the reference image and the obtained mask.

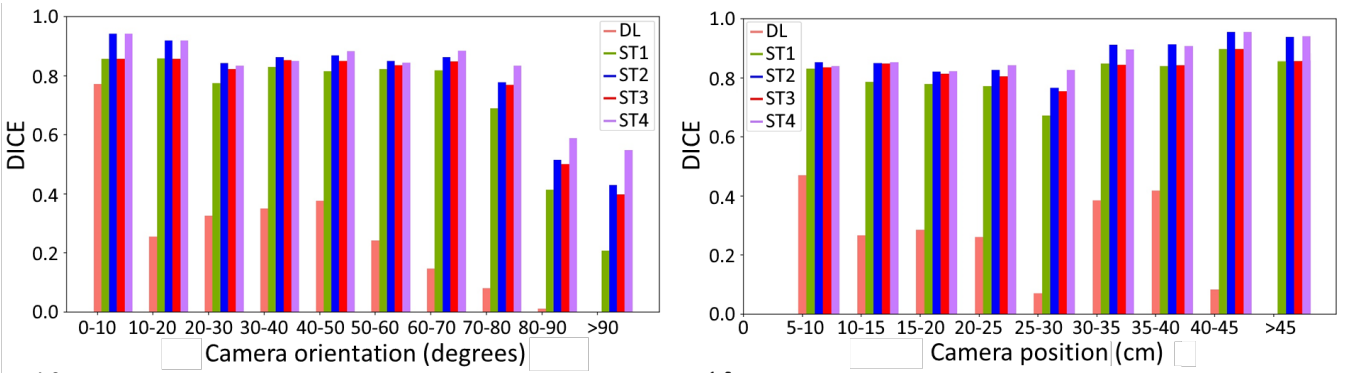

FIGURE 6. Calculated Dice coefficient across different angles and distances

The smaller the value of RMSE and MAE, the better the segmentation performance.

$$IoU = \frac{|X \cap Y|}{|X \cup Y|} \tag{1}$$

$$DICE = \frac{2 * |X \cap Y|}{|X| + |Y|} \tag{2}$$

$$RMSE(X,Y) = \sqrt{\frac{\sum_{i=1}^{n}(X_i - Y_i)^2}{n}} \tag{3}$$

$$MAE(X,Y) = \frac{\sum_{i=1}^{n}|X_i - Y_i|}{n} \tag{4}$$

where X and Y are the ground truth and the segmented mask, n is the total number of pixels in the image.

C. EXPERIMENTS AND ANALYSIS

To investigate the performance of the proposed method, we compared the segmentation results achieved by our 2D segmentation scheme including robust background elimination using Deep Learning (DL) against those obtained by including the 3D model with best view segmentation re-projection (BV+DL). In the following experiments, we consider the four different strategies introduced in Section III-D to choose effectively the best view for the proposed method. As a reminder, the best view in ST1, ST2, ST2 and ST4 is selected based on the best angle, the closest distance, the closest distance within the top 5 angles and the best angle among the 5 closest distances, respectively.

Dice and IoU were evaluated on DFU dataset across different angles and distances. Since the ulcer area in test images is much smaller than the background, these two metrics were measured locally to focus only on the segmented area. Figure 6 demonstrates that among all different angles and distances, the 2D method based on DL only, shows the worst segmentation performance according to DICE value compared to the proposed strategies. DL method can be greatly affected by viewing angle and distance. Starting with camera orientation, to obtain a good segmentation, the acquisition angle should be as perpendicular as possible to the wound bed, so closer to 0°. Bigger angle variation can result in lower segmentation accuracy. The best results were achieved for an angle variation less than 10°, what we call frontal views. Then DL performance started decreasing gradually the largest the angle value became. For an angle value over 80°, DICE was of 0%. Thus, DL method totally failed to detect the wound area in those images. Moreover, DL is rather sensitive to distance variation. The best segmentation was performed with a distance value between 5 and 10 cm. Otherwise, the method failed completely to segment the wound especially when the distance exceeds 40 cm.

TABLE 2. Area calculation (px)

		Area Calculation (px)				
Patient	Real_area	DL	ST1	ST2	ST3	ST4
Pat 1	514	385	**456**	**456**	**456**	**456**
Pat 2	4912	1629	**4835**	4194	3813	3813
Pat 3	59	11	**59**	**59**	58	57
Pat 4	94	8	91	91	91	**94**
Pat 5	359	293	**341**	**341**	**341**	**341**
Pat 6	51	0	29	**51**	**51**	42
Pat 7	324	227	297	**316**	297	**316**

However, reprojecting the segmentation from the BV using the 3D model helped to improve Dice across all angles and distance values regarding all proposed strategies. The performance of the obtained segmentation is much higher than DL. In addition, the results show high segmentation consistency among all points of view for the four strategies. Furthermore, ST2 and ST4 consistently outperforms other strategies. These two methods reached the highest Dice for the largest angles and farthest distances. Meanwhile, the metric using ST1 was lower than the other strategies but still better than DL.

Another interesting experiment to explore the effectiveness of the proposed strategies over DL method, is to quantify the number of detected pixels in the predicted mask. The results of wound area calculation in comparison with the real area corresponding to the ground truth for each patient were reported in Table 2. Overall, ST1, ST2, ST3 and ST4 produce high AC scores close to the RA of the ground truth according all patients and consistently outperforms DL scores. The four

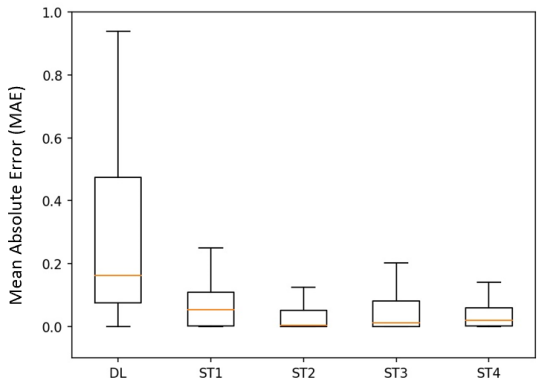

FIGURE 7. Box-plot of Mean Absolute Error

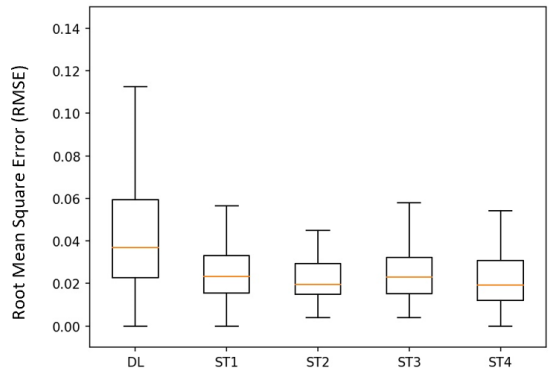

FIGURE 8. Box-plot of Root Mean Square Error

TABLE 3. A Summary of segmentation improvement

	Dice	IoU	MAE	RMSE
DL	36.53%	29.48%	0.164	0.036
ST1	83.49%	73.56%	0.054	0.023
ST2	**86.33%**	**77.09%**	**0.004**	**0.019**
ST3	84.52%	74.21%	0.012	0.023
ST4	85.40%	76.00%	0.020	0.020

strategies performed similarly but, in most of the cases, ST2 was the closest to the ground truth.

For further analysis, Figure 7 and Figure 8 illustrate the distribution of mean absolute error (MAE) and root mean square error (RMSE) respectively, between the ground truth mask and the obtained segmentation mask of each of the tested methods. The box-plots of DL method indicate larger MAE and RMSE resulting in lower segmentation quality. On the contrary, all BV+DL strategies show lower MAE and RMSE compared to DL. This correlates with higher segmentation accuracy. Moreover, we observe that ST2 attains the lowest MAE and RMSE in comparison to other strategies. These results corroborate our previous findings about ST2 performing better than ST1, ST3 and ST4.

Qualitative comparison of both methods DL and ST2 against the ground truth are shown in Figure 10. We chose image sequences of three patients with different DFU size

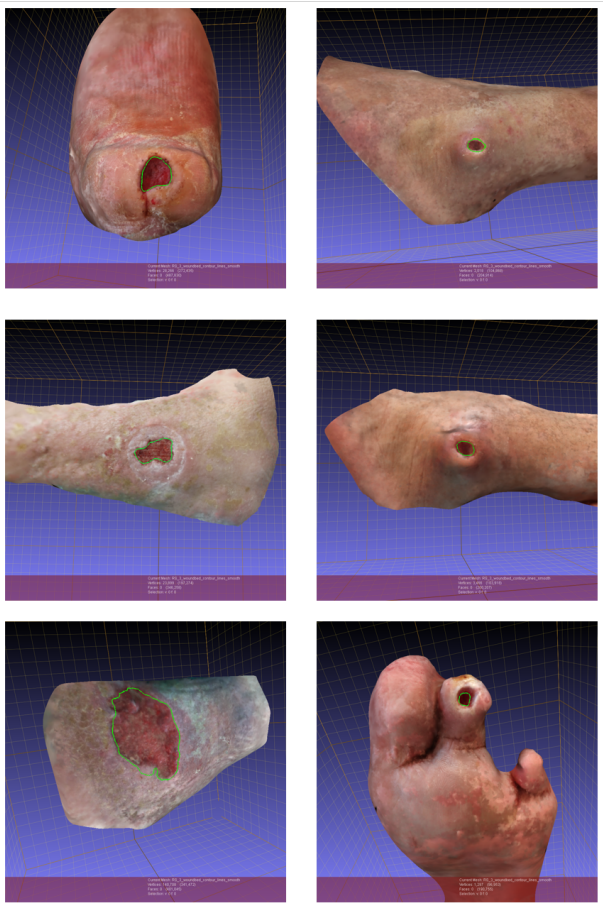

FIGURE 9. Segmentation results on the 3D model

(small, medium and big) to display our results. Really, the proposed method performs better to segment the ulcer. It successfully detected the wound area of different sizes and shapes regardless of camera position and orientation. The segmentation is much more accurate. In addition, the correct detection of the wound in case of deep learning failures is a statement of our method robustness.

Segmentation results on the 3D model are shown on Figure 9. These results are obtained by the fusion of single view segmentation masks. To do this, first we performed wound segmentation on each image of the multi-view sequence, then these results are directly mapped on the mesh surface of the 3D model.

V. DISCUSSION

Comparing quantitative and qualitative results of the 2D method based on single view DL segmentation and the proposed method based on 3D model reconstruction and best view segmentation reprojection, we can see a huge improvement on metrics and segmentation quality. By comparing different strategies to select effectively the best view, we found out that ST2 performed the best and achieved the highest performance. It has not only better accuracy, but also

FIGURE 10. Segmentation results: (a) original images, (b) Ground truth, (c) output of DL method and (d) output of our method

better robustness. This strategy consists on selecting the view with the best distance.

Our method widely improved both Dice and IoU scores and decreased segmentation error on test dataset (See Table 3). The obtained contours outline perfectly the wound area. Thus, the proposed method not only overcomes the limitations of DL due to wound size and location, but also guarantees a precise segmentation among different shooting angles and distances in the image sequence. However, despite the high segmentation accuracy using the BV reprojection, the segmentation performance drop significantly once rotation angle exceeds 80° for all proposed strategies.

VI. CONCLUSION

In this paper, we attempted to solve weak DL segmentation accuracy problem due to camera position and shooting angles during multi-view wound acquisition. A smartphone was used to capture the wound from multiple views which is cost-effective, user-friendly and harmless. Our approach improves DL segmentation using the 3D model and best view selection. Comprehensive experiments have demonstrated the effectiveness of our method in comparison with single view DL segmentation, the result is a robust segmentation in all the views regardless of camera position and orientation. Therefore, the proposed method is used as an effective weakly supervised data augmentation approach to deal with the lack of annotated data in medical field using real images that encompass all real aspects of the wound from different viewing perspectives.

The obtained segmentation masks are also used to generate the final segmentation of the wound in the 3D model. A future research would be to use the 3D model for depth and volume estimation to overcome the shortcomings of 2D methods based on single view especially for highly curved wounds. Moreover, we plan to extend our method to perform multi-view tissue classification considering three classes (granulation, slough and necrosis) using the 3D representation of the wound to achieve a more robust tissue analysis. Thus, more accurate assessment could be established including wound area, depth and volume as well as tissue characterization. Such a system can be used in clinical settings for all kinds of chronic wounds regardless of their size, shape and location.

ACKNOWLEDGMENT

The authors express their gratitude to the European Union's Horizon 2020 under the Marie Sklodowska-Curie grant agreement No 777661 for their financial support.

REFERENCES

[1] C. E. Fife, K. A. Eckert, and M. J. Carter, "Publicly reported wound healing rates: the fantasy and the reality," *Advances in wound care*, vol. 7, no. 3, pp. 77–94, 2018.
[2] C. Little, J. McDonald, M. Jenkins, and P. McCarron, "An overview of techniques used to measure wound area and volume," *Journal of wound care*, vol. 18, no. 6, pp. 250–253, 2009.
[3] D. Langemo, J. Anderson, D. Hanson, S. Hunter, and P. Thompson, "Measuring wound length, width, and area: which technique?" *Advances in skin & wound care*, vol. 21, no. 1, pp. 42–45, 2008.
[4] C. Ahn *et al.*, "Advances in wound photography and assessment methods," *Advances in skin & wound care*, vol. 21, no. 2, pp. 85–93, 2008.
[5] L. B. Jørgensen, J. A. Sørensen, G. B. Jemec, and K. B. Yderstræde, "Methods to assess area and volume of wounds–a systematic review," *International wound journal*, vol. 13, no. 4, pp. 540–553, 2016.
[6] S. M. Nagle, A. Waheed, and S. C. Wilbraham, "Wound assessment," *StatPearls [Internet]*, 2020.
[7] Y. Lucas, R. Niri, S. Treuillet, H. Douzi, and B. Castaneda, "Wound size imaging: Ready for smart assessment and monitoring," *Advances in wound care*, 2020.
[8] O. H. Karatas and E. Toy, "Three-dimensional imaging techniques: A literature review," *European journal of dentistry*, vol. 8, no. 1, p. 132, 2014.
[9] D. H. Keast, C. K. Bowering, A. W. Evans, G. L. Mackean, C. Burrows, and L. D'Souza, "Contents: Measure: A proposed assessment framework for developing best practice recommendations for wound assessment," *Wound Repair and Regeneration*, vol. 12, pp. s1–s17, 2004.
[10] P. Gholami, M. A. Ahmadi-Pajouh, N. Abolftahi, G. Hamarneh, and M. Kayvanrad, "Segmentation and measurement of chronic wounds for bioprinting," *IEEE journal of biomedical and health informatics*, vol. 22, no. 4, pp. 1269–1277, 2017.
[11] C. Liu, X. Fan, Z. Guo, Z. Mo, I. Eric, C. Chang, and Y. Xu, "Wound area measurement with 3d transformation and smartphone images," *BMC bioinformatics*, vol. 20, no. 1, pp. 1–21, 2019.
[12] C. Wang, D. Anisuzzaman, V. Williamson, M. K. Dhar, B. Rostami, J. Niezgoda, S. Gopalakrishnan, and Z. Yu, "Fully automatic wound segmentation with deep convolutional neural networks," *Scientific Reports*, vol. 10, no. 1, pp. 1–9, 2020.
[13] G. Blanco, A. J. Traina, C. Traina Jr, P. M. Azevedo-Marques, A. E. Jorge, D. de Oliveira, and M. V. Bedo, "A superpixel-driven deep learning approach for the analysis of dermatological wounds," *Computer methods and programs in biomedicine*, vol. 183, p. 105079, 2020.
[14] D. Y. Chino, L. C. Scabora, M. T. Cazzolato, A. E. Jorge, C. Traina-Jr, and A. J. Traina, "Segmenting skin ulcers and measuring the wound area using deep convolutional networks," *Computer methods and programs in biomedicine*, vol. 191, p. 105376, 2020.
[15] S. Zahia, B. Garcia-Zapirain, and A. Elmaghraby, "Integrating 3d model representation for an accurate non-invasive assessment of pressure injuries with deep learning," *Sensors*, vol. 20, no. 10, p. 2933, 2020.
[16] H. Wannous, Y. Lucas, and S. Treuillet, "Enhanced assessment of the wound-healing process by accurate multiview tissue classification," *IEEE transactions on Medical Imaging*, vol. 30, no. 2, pp. 315–326, 2010.
[17] F. J. Veredas, R. M. Luque-Baena, F. J. Martín-Santos, J. C. Morilla-Herrera, and L. Morente, "Wound image evaluation with machine learning," *Neurocomputing*, vol. 164, pp. 112–122, 2015.
[18] L. Wang, P. C. Pedersen, E. Agu, D. M. Strong, and B. Tulu, "Area determination of diabetic foot ulcer images using a cascaded two-stage svm-based classification," *IEEE Transactions on Biomedical Engineering*, vol. 64, no. 9, pp. 2098–2109, 2016.
[19] L. Alzubaidi, M. A. Fadhel, S. R. Oleiwi, O. Al-Shamma, and J. Zhang, "Dfu_qutnet: diabetic foot ulcer classification using novel deep convolutional neural network," *Multimedia Tools and Applications*, vol. 79, no. 21, pp. 15 655–15 677, 2020.
[20] M. Goyal, N. D. Reeves, S. Rajbhandari, and M. H. Yap, "Robust methods for real-time diabetic foot ulcer detection and localization on mobile devices," *IEEE journal of biomedical and health informatics*, vol. 23, no. 4, pp. 1730–1741, 2018.
[21] M. Tan, R. Pang, and Q. V. Le, "Efficientdet: Scalable and efficient object detection," in *Proceedings of the IEEE/CVF conference on computer vision and pattern recognition*, 2020, pp. 10 781–10 790.
[22] B. Cassidy, N. D. Reeves, P. Joseph, D. Gillespie, C. O'Shea, S. Rajbhandari, A. G. Maiya, E. Frank, A. Boulton, D. Armstrong *et al.*, "Dfuc2020: Analysis towards diabetic foot ulcer detection," *arXiv preprint arXiv:2004.11853*, 2020.
[23] M. Goyal and S. Hassanpour, "A refined deep learning architecture for diabetic foot ulcers detection," *arXiv preprint arXiv:2007.07922*, 2020.
[24] M. H. Yap, R. Hachiuma, A. Alavi, R. Brungel, M. Goyal, H. Zhu, B. Cassidy, J. Ruckert, M. Olshansky, X. Huang *et al.*, "Deep learning in diabetic foot ulcers detection: A comprehensive evaluation," *arXiv preprint arXiv:2010.03341*, 2020.
[25] Y. Yu, H. Lin, J. Meng, X. Wei, H. Guo, and Z. Zhao, "Deep transfer learning for modality classification of medical images," *Information*, vol. 8, no. 3, p. 91, 2017.
[26] F. L. Bowling, L. King, H. Fadavi, J. A. Paterson, K. Preece, R. W. Daniel, D. J. Matthews, and A. J. M. Boulton, "An assessment of the accuracy

and usability of a novel optical wound measurement system," *Diabetic Medicine*, vol. 26, no. 1, pp. 93–96, Jan. 2009. [Online]. Available: http://doi.wiley.com/10.1111/j.1464-5491.2008.02611.x
[27] L. B. Jørgensen, U. Halekoh, G. B. Jemec, J. A. Sørensen, and K. B. Yderstræde, "Monitoring Wound Healing of Diabetic Foot Ulcers Using Two-Dimensional and Three-Dimensional Wound Measurement Techniques: A Prospective Cohort Study," *Advances in Wound Care*, vol. 9, no. 10, pp. 553–563, Oct. 2020. [Online]. Available: https://www.liebertpub.com/doi/10.1089/wound.2019.1000
[28] M. Malone, S. Schwarzer, A. Walsh, W. Xuan, A. Al Gannass, H. G. Dickson, and F. L. Bowling, "Monitoring wound progression to healing in diabetic foot ulcers using three-dimensional wound imaging," *Journal of Diabetes and its Complications*, vol. 34, no. 2, p. 107471, Feb. 2020. [Online]. Available: https://linkinghub.elsevier.com/retrieve/pii/S1056872719310050
[29] F. Zvietcovich, B. Castaneda, B. Valencia, and A. Llanos-Cuentas, "A 3D assessment tool for accurate volume measurement for monitoring the evolution of cutaneous Leishmaniasis wounds," in *2012 Annual International Conference of the IEEE Engineering in Medicine and Biology Society*. San Diego, CA: IEEE, Aug. 2012, pp. 2025–2028. [Online]. Available: http://ieeexplore.ieee.org/document/6346355/
[30] E. S. Darwin, J. A. Jaller, P. A. Hirt, and R. S. Kirsner, "Comparison of 3-dimensional Wound Measurement With Laser-assisted and Hand Measurements: A Retrospective Chart Review," *Wound Management & Prevention*, vol. 65, no. 1, pp. 36–41, Jan. 2019. [Online]. Available: https://www.o-wm.com/article/comparison-3-dimensional-wound-measurement-laser-assisted-and-hand-measurements
[31] S. Treuillet, B. Albouy, and Y. Lucas, "Three-Dimensional Assessment of Skin Wounds Using a Standard Digital Camera," *IEEE Transactions on Medical Imaging*, vol. 28, no. 5, pp. 752–762, May 2009. [Online]. Available: http://ieeexplore.ieee.org/document/4749314/
[32] O. Zenteno, E. Gonzalez, S. Treuillet, B. M. Valencia, B. Castaneda, A. Llanos-Cuentas, and Y. Lucas, "Volumetric monitoring of Leishmaniasis ulcers: Can camera be as accurate as laser scanner for treatment monitoring?" p. 13.
[33] L. Casas, S. Treuillet, B. Valencia, A. Llanos, and B. Castañeda, "Low-cost uncalibrated video-based tool for tridimensional reconstruction oriented to assessment of chronic wounds," E. Romero and N. Lepore, Eds., Cartagena de Indias, Colombia, Jan. 2015, p. 928711. [Online]. Available: http://proceedings.spiedigitallibrary.org/proceeding.aspx?doi=10.1117/12.2070995
[34] P. Ondruska, P. Kohli, and S. Izadi, "MobileFusion: Real-Time Volumetric Surface Reconstruction and Dense Tracking on Mobile Phones," *IEEE Trans. Visual. Comput. Graphics*, vol. 21, no. 11, pp. 1251–1258, Nov. 2015. [Online]. Available: https://ieeexplore.ieee.org/document/7165662/
[35] O. Muratov, Y. Slynko, V. Chernov, M. Lyubimtseva, A. Shamsuarov, and V. Bucha, "3DCapture: 3D Reconstruction for a Smartphone," in *2016 IEEE Conference on Computer Vision and Pattern Recognition Workshops (CVPRW)*. Las Vegas, NV, USA: IEEE, Jun. 2016, pp. 893–900. [Online]. Available: http://ieeexplore.ieee.org/document/7789606/
[36] N. Rania, H. Douzi, L. Yves, and T. Sylvie, "Semantic segmentation of diabetic foot ulcer images: Dealing with small dataset in dl approaches," in *Image and Signal Processing*, A. El Moataz, D. Mammass, A. Mansouri, and F. Nouboud, Eds. Cham: Springer International Publishing, 2020, pp. 162–169.
[37] O. Ronneberger, P. Fischer, and T. Brox, "U-net: Convolutional networks for biomedical image segmentation," in *International Conference on Medical image computing and computer-assisted intervention*. Springer, 2015, pp. 234–241.
[38] K. Sreedhar and B. Panlal, "Enhancement of images using morphological transformation," *arXiv preprint arXiv:1203.2514*, 2012.
[39] D. P. Kingma and J. Ba, "Adam: A method for stochastic optimization," *arXiv preprint arXiv:1412.6980*, 2014.
[40] AliceVision, "Meshroom: A 3D reconstruction software." 2018. [Online]. Available: https://github.com/alicevision/meshroom

R. NIRI received the MS degree in Big Data and Cloud computing from Hassan II University, Morocco, in 2017. Since 2018, she is a PhD student in computer vision and medical image analysis at IRF-SIC Laboratory, Ibn Zohr University, Morocco and PRISME Laboratory, Orleans University, France. Her research interests focus on artificial intelligence applied to medical image processing using deep learning methods for optical wound assessment including wound segmentation and tissue classification.

E. GUTIERREZ received her MS in Statistics from Pontificia Universidad Católica del Perú in 2016 and BSC from the National University of Engineering, Peru. Currently, Evelyn is pursuing a PhD in Engineering in co-supervision between Pontificia Universidad Católica del Perú, Peru and the University of Orleans, France. Her research focuses on wound monitoring using multimodal imaging and portable devices.

H. DOUZI received the PhD degree in Applied Mathematics from Paris IX University (Dauphine), France in 1992. Since 1993, he has been a research professor at Ibn-Zohr University, Agadir in Morocco. He is currently the head of the IRF-SIC laboratory in the same university. His research interests include wavelet analysis and image processing applications as well as information processing methods in general.

Y. LUCAS received his MS degree in discrete mathematics from Lyon University, France, in 1988, and the PhD degree from the National Institute of Applied Sciences in Lyon, France in 1993. He is an associate professor at PRISME laboratory, Orleans University, France, in charge of the Image and Vision Team activities covering3D geometrical modelling, multimodal imaging and video analysis. His research interests focus on medical applications such as optical wound assessment, tissue detection, hyperspectral endoscopy and patient care monitoring for orthodontics.

S. TREUILLET received the master's degree in electrical engineering from the University of Clermont-Ferrand, France, in 1988, and the Ph.D. degree in computer vision from the University of Clermont-Ferrand, France, in 1993. Since 1994, she has been an Assistant Professor of Computer Sciences and Electronic Engineering with the Ecole Polytechnique and with the PRISME Laboratory, University of Orléans, France. Her research interests include computer vision for 3-D object modeling, pattern recognition, and color image analysis for biomedical or industrial applications.

B.CASTANEDA received the B.S. degree in electronics engineering from the Pontificia Universidad Católica del Perú (PUCP), Lima, Peru, in 2000, the M.S. degree in computer engineering from the Rochester Institute of Technology, Rochester, NY, USA, in 2004, and the M.S. and Ph.D. degrees in electrical and computer engineering from the University of Rochester in 2006 and 2009, respectively.He is currently the Chair of the Biomedical Engineering Program at PUCP.

DR. I. HERNANDEZ is a plastic surgeon with 20 years of experience in tissue engineering, with an emphasis on soft tissue repair through the use of bioactive molecules, scaffolds, and adult stem cells. He is member of American Society of plastic surgeons and Sociedad Peruana de Cirugía Plastica and International Society for Cellular therapy. He is a professor and researcher at the Instituto de investigaciones de ciencias biomédicas, facultad de medicina of Universidad Ricardo Palma, where he manages the regenerative medicine research line and is a consultant in tissue engineering for the plastic surgery service of the Hospital Hipólito Unanue in Lima, Peru.